Desalination and Water Treatment
www.deswater.com

doi: 10.5004/dwt.2019.24007

154 (2019) 254–267
June

Methyl tertiary-butyl ether adsorption by bioactivated carbon from aqueous solution: kinetics, isotherm and artificial neural network modeling

Ali Fatehizadeh[a,b], Mohammad Reza Zare[c], Steven W Van Ginkel[d], Ensiyeh Taheri[a,b], Mohammad Mehdi Amin[a,b,*], Nasim Rafiei[a,b], Mokhtar Mahdavi[e,f]

[a]*Department of Environmental Health Engineering, School of Health, Isfahan University of Medical Sciences, Isfahan, Iran, Tel. +98 313 792 3276; Fax: +98 313 669 5849; emails: amin@hlth.mui.ac.ir (M.M. Amin), fatehizadeh@gmail.com, a.fatehizadeh@hlth.mui.ac.ir (A. Fatehizadeh), e_taheri_83@yahoo.com (E. Taheri), nasim.rafiei@hlth.mui.ac.ir (N. Rafiei)*
[b]*Environment Research Center, Research Institute for Primordial Prevention of Non-communicable Disease, Isfahan University of Medical Sciences, Isfahan, Iran*
[c]*Department of Environmental Health Engineering, School of Health, Larestan University of Medical Sciences, Larestan, Iran, email: zaremohammad1363@yahoo.com*
[d]*School of Civil and Environmental Engineering, Georgia Institute of Technology, 200 Boddy Dodd Way, Atlanta, GA 30332 USA, email: svg7@mail.gatech.edu*
[e]*Social Determinates of Health Research Center, Saveh University of Medical Sciences, Saveh, Iran, email: shamall6@yahoo.com*
[f]*Student Research Committee of Saveh University of Medical Sciences, Saveh, Iran*

Received 17 October 2018; Accepted 20 February 2019

ABSTRACT

The present study evaluated fabrication of bioactivated carbon (BAC) from waste activated sludge (WAS) for methyl tert-butyl ether (MTBE) removal from aqueous solution. BACs were prepared using KOH, H_3PO_4, and $ZnCl_2$ as chemical activation reagents, followed by thermal activation. Batch experiments with different BAC types and dosages, solution pH, initial MTBE concentrations, and contact times were conducted to investigate the BAC effectiveness. The obtained data were analyzed using the kinetics and isotherm model and also with artificial neural network (ANN). The result of Fourier transform infrared (FTIR) spectra of WAS and BAC was depicted that the C–H and C–C were major surface functional groups. The $ZnCl_2$ activated carbon had the highest adsorption capacity for MTBE adsorption, followed by H_3PO_4 and KOH activated carbons. The results showed that the highest MTBE removal was observed at solution pH equal to 4 and approximately 30% of MTBE could be adsorbed with 30 min contact time. It was also found that MTBE adsorption followed the R–P isotherm and pseudo-second order (type 1) kinetic models. During ANN modeling, the optimum neurons number for Levenberg–Marquardt training algorithm was determined equal to 5 with highest R^2 value and lowest mean square error were found to be 0.99 and 5.7×10^{-4}, respectively.

Keywords: Activated carbon; Chemical activation; Thermal activation

1. Introduction

Due to their toxic and/or carcinogenic properties, petroleum hydrocarbons represent one of the most common categories of groundwater pollutants found at contaminated sites, making surface water and/or groundwater unsuitable for many uses. Since 1970s, methyl tert-butyl ether (MTBE) was developed as an organic solvent in the chemical industry and as an anti-knocking agent and octane-enhancing gasoline additive to replace tetra-ethylene lead [1]. The high water solubility (43–54 g/L) and low Henry's law constant (0.023–0.12; dimensionless) make MTBE mobile and persistent in water [2]. Some MTBE removal processes from

* Corresponding author.

water include advanced oxidation [3], electrochemical removal [4], solvent impregnated resins [5], adsorption [6], air stripping [5], and bioremediation [7]. In addition, MTBE is fairly resistant to biodegradation and chemical oxidation, and these processes may lead to the formation of undesirable metabolites or oxidation intermediates such as tert-butyl alcohol [8].

Adsorption is a mass transfer process in which a contaminant in a liquid or gas phase is transferred into a solid or liquid phase [9]. Adsorption is an excellent technology in which petroleum hydrocarbons can be concentrated onto an adsorbent mass. The adsorption can be used for MTBE removal either in-situ (in permeable reactive barriers) or ex-situ (in combination with pump-and-treat systems) [10]. Due to its simple design, lack of sludge production, and low investment costs, the adsorption process has more advantages than other methods in removing pollutants from water and wastewater. Granular activated carbon [11], polymeric adsorbents [12], zeolite [13], lignite [14], and synthetic resins [15] are among some adsorbents that have been used for MTBE removal.

Activated carbon can be obtained by both chemical and physical activation of precursor material [16]. This means that during chemical activation, where the activating agent is a dehydrating compound, there will be an increase in activated carbon yield and the thermal degradation of the precursor which increases the porosity of activated carbon [17].

The increasing generation of sewage sludge derived from wastewater treatment demands the development of new ways for its disposal or recycling. Some authors have investigated the direct application of dried sewage sludge as an adsorbent but have observed some limitations [16]. One of the adsorbents that can be attained from sewage sludge is activated carbon (known as bioactivated carbon [BAC]). Owing to its low initial cost, simplicity of design, insensitivity to toxic substances, high adsorption capacity, and re-generability, activated carbon appears to be the most versatile and suitable candidate for the removal of contaminants from water. This fact has motivated a noticeable interest for the development of carbon-based adsorbents from many different precursors for industrial applications [16].

1.1. Artificial neural networks

Nowadays, application of artificial neural network (ANN) models is extensive and used to examine relationships in complex nonlinear data sets. ANN models have gained acceptance in numerous engineering fields as they provide spontaneous learning from examples and produce adequate and rapid responses to new information. ANNs have been mainly consisted of three layers: input layer, hidden layer, and output layers. The models run with interaction of elementary processing units (neurons) by sending signals to one another along weighted connections. In the system each neuron is connected to all neurons in the preceding and following layer by links [18].

Each input value is represented by a neuron in the input layer. Input values are weighted individually before entering the hidden layer and weighted values are transferred to the hidden layer. In the hidden layer each neuron produces outputs based on the sum of the weighted values from the input layer. Outputs of a neuron can be calculated according to Eq. (1).

$$o = f\left(\sum_{j=0}^{n} \omega_{ij} \times x_j\right) \tag{1}$$

where n represents the number of inputs, x_j is the j^{th} input to the neuron, ω_j is the j^{th} synaptic weight, and f is a non-linear function [19].

In the study, hyperbolic tangent function that produces outputs between −1 and +1 was preferred (Eq. (2)).

$$\tanh(x) = \frac{2}{1+e^{-2x}} - 1 \tag{2}$$

In training process run with a data set of input and output data, weights of the network are adjusted to obtain the similar outputs as seen in the training data set. With this aim, data were divided into the two subsets for training and model validation purposes.

In order to avoid numerical overflows due to very large or small weights, all of the data were converted to normalized values by using Eq. (3).

$$x_{\text{norm}} = 0.8 \times \left(\frac{x_i - x_{\min}}{x_{\max} - x_{\min}}\right) + 0.1 \tag{3}$$

Performances of the developed models were evaluated by considering mean standard error (MSE) value and Pearson coefficient (r^2) with Eqs. (4) and (5), respectively [20].

$$\text{MSE} = \frac{1}{N}\sum_{i=1}^{N}\left(\left|y_{\text{pre},i} - y_{\text{exp},i}\right|\right)^2 \tag{4}$$

$$r^2 = 1 - \frac{\sum_{i=1}^{N}\left(y_{\text{pre},i} - y_{\text{exp},i}\right)^2}{\sum_{i=1}^{N}\left(y_{\text{pre},i} - y_{\text{ave}}\right)^2} \tag{5}$$

However, no study has investigated the application of activated carbon derived from sewage sludge as a raw material for MTBE removal. This research attempts to study the preparation of activated carbon from waste activated sludge (WAS) for the removal of MTBE from aqueous solution.

2. Materials and methods

2.1. BAC preparation and properties

The WAS came from the return sludge line before sludge processing facilities of a biological wastewater treatment plant (Isfahan south wastewater treatment plant, Isfahan, Iran) was used as the raw material for the production of activated carbon. The sludge had solid content of 1%, pH of 7.4 suspended solids concentration of 9.4 g/L and volatile solids concentration of 7.5 g/L. Elemental composition of the WAS was as follows: C, 36.7; H, 6.9; N, 7.8; O, 9.9; Ca, 13.9; Si, 9.1; Fe, 4.2; Al, 2.9; S, 2.8; P, 2.4; K, 1.2; Mg, 0.89; Ti, 0.38; Zn, 0.24;

Cl, 0.22; Na, 0.19; Cu, 0.17; Sr, 0.11; Mn, 0.07; as %W/W. Also, loss on ignition (at 1,000°C, 2 h) was 61.25 (%W/W). Fig. 1 shows a schematic representation of the fabrication of BAC from WAS. Three BACs were produced and tested. BACs#1, #2, and #3 were chemically activated using H_3PO_4, KOH, and $ZnCl_2$, respectively.

2.2. Chemicals and instrumentation

The chemicals tested in this study were sulfuric acid, phosphoric acid, zinc chloride, potassium hydroxide, and MTBE. All chemicals were of analytical grade and obtained from Merck Co., Germany. The MTBE and C, H, N, and O amounts were determined by Agilent gas chromatography and ECS 4010 CHNOS analyzer, respectively.

2.3. Batch experiment

All experiments were carried out in batch systems using air tight flasks at 25°C and an agitation speed of 200 rpm using an orbital shaker. The flasks were filled with 50 mL of MTBE solution with different initial MTBE concentrations, solution pH, and amounts of BAC. A summary of experimental conditions employed for MTBE adsorption is presented in Table 1.

Upon completion of the reaction time, samples were filtered (Whatman No. 1) and the MTBE concentrations were analyzed. To promote the accuracy of adsorption tests, all experiments were done with excess control flasks. MTBE removal efficiency and absorption capacity were calculated using Eqs. (6) and (7), respectively.

$$E_r = \left[\frac{C_0 - C_e}{C_0}\right] \times 100 \tag{6}$$

$$q_e = \frac{C_0 - C_e}{m} \times V \tag{7}$$

2.4. Chemical analysis

The residual MTBE concentration in the liquid phase after the adsorption process was determined using MTBE's Henry's constant and by measuring MTBE in the gas phase using an Agilent gas chromatography outfitted with a flame ionization detector. The temperatures of the injector and detector were 150°C and 250°C, respectively. The column oven temperature was initially held at 40°C for 10 min, then increased at a rate of 10°C/min to a maximum 150°C, and then held for 10 min. Helium and nitrogen were used at flow rates of 1 and 30 mL/min as the carrier and make-up gases, respectively. A capillary column was used (Cp.Sil 5 Cb, 25 m × 320 μm × 1.2 μm) and was purchased from the United States. Gas analysis in the head space was sampled using a CombiPal system. The vials were incubated at 70°C with 1 min mixing at 500 rpm with a 250 μL injection volume. Also, the composition of the activated sludge including C, H, O, N, and S amount was determined using ECS 4010 CHNOS Analyzer.

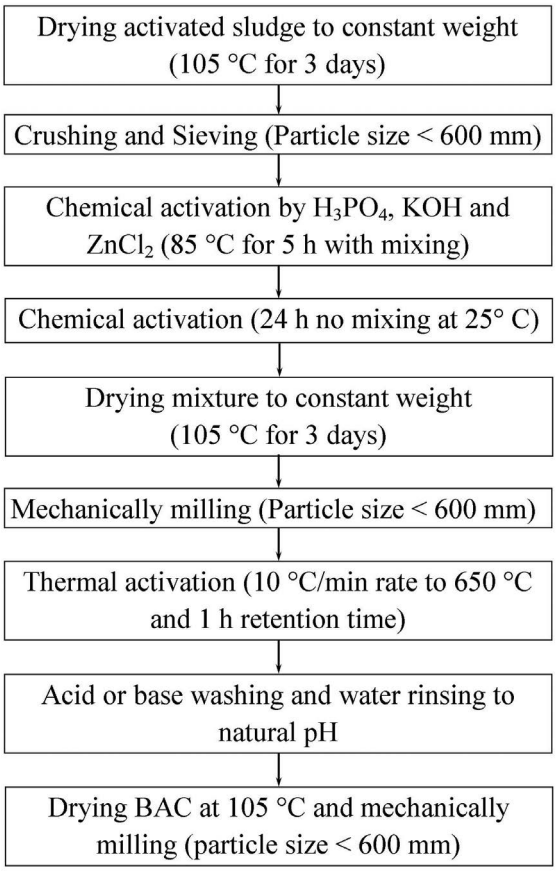

Fig. 1. Schematic representation of BAC fabrication from WAS.

Table 1
Experimental conditions employed in MTBE adsorption by BAC

Studied parameter	Experimental conditions				
	MTBE concentration (mg/L)	Solution pH	Adsorption dose (g/L)	Contact time (min)	BAC type
Adsorbent type	70	7	2–4	60	BAC#1, 2 and 3
Solution pH	70	2–10	3	60	BAC#3
Contact time	20–60	4	5	0–240	BAC#3
BAC dose	20–70	4	2–7	240	BAC#3
Initial MTBE concentration	20–70	4	2–7	240	BAC#3

2.5. Statistical analyses

Differences between BAC chemical activations, initial MTBE concentrations, and BAC dose were examined using one-way ANOVA. All calculations were performed through the use of SPSS version 16 for windows.

3. Results and discussion

3.1. Characterization of BAC

The Fourier transform infrared (FTIR) spectra can provide valuable information about the chemical composition of materials. The FTIR spectra of WAS and BAC at wave numbers ranging from 400 to 4,000 cm^{-1} are depicted in Fig. 2. The IR bands at 3,299 cm^{-1} is characteristic of the C–H stretching vibration from aromatic rings. IR bands at 2,959; 2,920; 2,851; and 2,513 cm^{-1} are assigned to the C–H stretching vibration from alkyl groups. IR bands at 1,540; 1,434; and 1,230 cm^{-1}, characteristic of aromatic C–C and alkyl C–H vibrations, were also visible. Aromatic C–H vibrations were evidenced by IR bands at 874, 799, and 711 cm^{-1}. Additional bands at 526 and 468 cm^{-1} can be assigned to typical O–Si–O and bending vibrations.

The scanning electron microscopy (SEM) was used for BAC#3 surface observation, and BAC#3 micrograph is depicted in Fig. 3. As seen in Fig. 3, the micrographs was contain the different sizes and shapes of pores, which resulted from the evaporation of $ZnCl_2$ (chemical reagents) during carbonization.

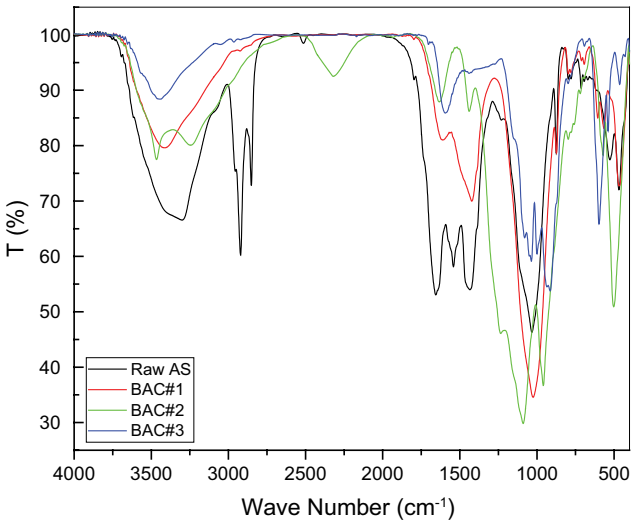

Fig. 2. FTIR spectra of raw activated sludge and BAC.

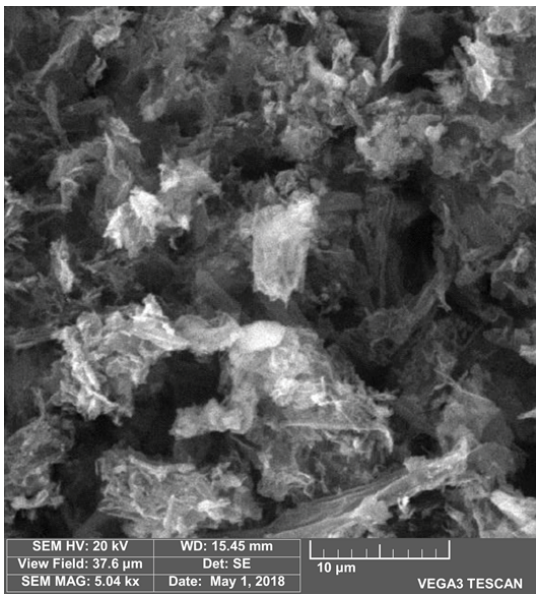

Fig. 3. SEM pictures of BAC#3.

3.2. Batch adsorption experiments

3.2.1. Adsorbent type

Fig. 4a shows the absorption capacity of BAC in MTBE adsorption under mentioned conditions. According to Fig. 4a, the chemical activation of WAS has a promoted influence on MTBE adsorption. MTBE adsorption capacities of 6.05 ± 1.13, 5.66 ± 0.77, and 7.12 ± 1.52 mg/g were obtained for the BACs#1, 2, and 3, respectively. The differences between adsorption capacities of the three BAC types were statistically examined by one-way ANOVA. No significant difference in adsorption capacities was observed between the three BAC types (p-value > 0.36). Due to the higher adsorption capacity of BAC#3 (7.12 ± 1.52 mg/g), BAC#3 was chosen for future adsorption experiments.

3.2.2. Effect of pH value on MTBE adsorption

In the adsorption process, solution pH has a direct influence on the chemical and physical properties of both the adsorbent and the adsorbate [9,21]. The effect of solution pH on the removal efficiency of MTBE was studied using 70 mg/L of MTBE and 3.0 g/L of BAC#3 at different solution pH values (2.0–10). Fig. 4b compares the effect of the solution pH on MTBE removal efficiency. As seen in Fig. 4b, with increasing solution pH from 2 to 4, the MTBE removal improved. A further increase in solution pH decreased MTBE removal efficiency; the weak positive charge of non-polarity compounds (such as MTBE) is maximum at lower pHs, and the surface charge can be decreased rapidly by increasing the pH [6]. The maximum MTBE removal efficiency was obtained at solution pH 4 and the results were in line with MTBE removal by modified natural zeolites (solution pH equal to 4) [1].

3.2.3. Effect of contact time on MTBE removal

The influence of contact time on MTBE removal efficiency was performed by shaking 5 g/L of BAC#3 in solution with 20, 40, and 60 mg/L of MTBE and a constant pH (4 ± 0.1). Fig. 4c illustrates the results of the contact time effect on MTBE removal. According to the results, MTBE removal increased with contact time. The influence of contact time is more pronounced at the early stage of the adsorption process – around 20% of MTBE removal occurred in the first 5–20 min (Fig. 4c), and thereafter the rate of adsorption of MTBE onto BAC#3 was found to be slow.

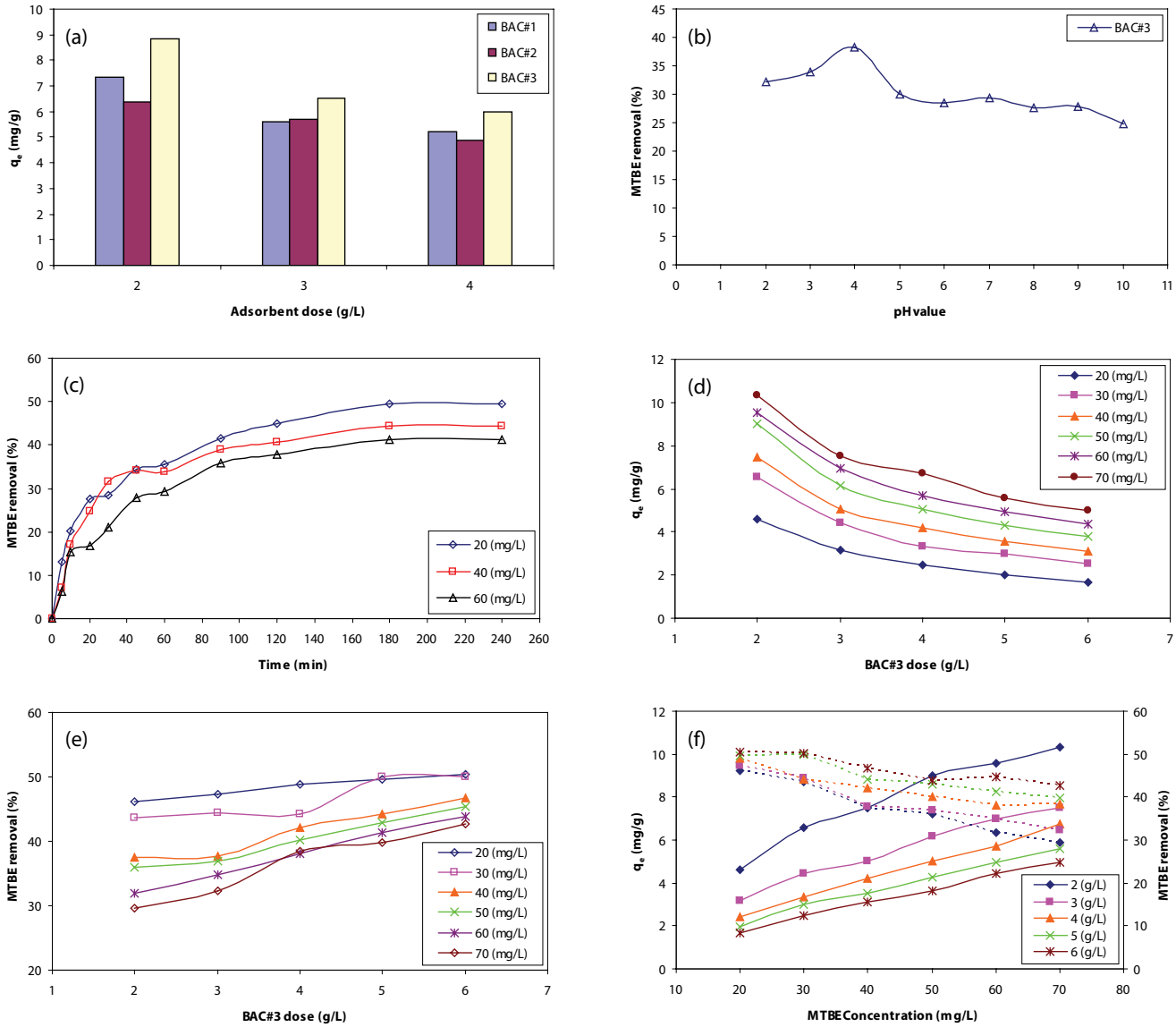

Fig. 4. MTBE removal at different experimental conditions: (a) adsorption behavior of MTBE by different adsorbents, (b) variation of MTBE adsorption onto BAC #3 as function of solution pH, (c) effect of contact time on the removal of initial MTBE concentrations using BAC #3, effect of BAC #3 dose on (d) absorption capacity (q_e) and (e) MTBE removal, (f) effect of initial concentration of MTBE on MTBE removal and q_e.

This first rapid adsorption is related to the concentration gradient created between MTBE in solution and the BAC#3 surface. The equilibrium contact time was found to be nearly 240 min when the maximum MTBE adsorption onto BAC3# was reached and was equal to 1.9, 3.5, and 4.9 mg/g at initial MTBE concentrations of 20, 40, and 60 mg/L, respectively. A significant difference was observed between effluent MTBE concentrations after the adsorption process using BAC#3 at different contact times (p-value <0.05).

3.2.4. *Effect of BAC#3 dose on MTBE adsorption*

The adsorbent dose is an important parameter in the adsorption process because it determines the adsorbent capacity of a given initial adsorbate concentration. The effect of BAC#3 dose on MTBE removal was studied using different masses of adsorbent (2–6 g/L) and initial MTBE concentrations (20–70 mg/L) at pH 4. Results are presented in Figs. 4d and e as MTBE adsorption capacity (mg/g) and MTBE removal efficiency (%), respectively, as functions of adsorbent dose. Adsorption capacity declined with increasing BAC#3 doses. At the lowest initial MTBE concentration (20 mg/L), the adsorption capacity decreased from 4.1 to 1.7 mg/g as the BAC#3 dosage was increased from 2 to 6 g/L (Fig. 4d).

An increase in the amount of BAC#3 increased MTBE removal. The MTBE removal efficiency increased as the adsorbent dose was increased from 2 to 6 g/L for all initial MTBE concentrations (Fig. 4e).

3.2.5. Effect of initial MTBE concentration

In order to determine the influence of the initial MTBE concentration on absorption, batch adsorption experiments were carried out using BAC #3 dosages of 2–6 g/L and initial MTBE concentrations of 20–70 mg/L at pH 4. MTBE removal and absorption capacities are shown in Fig. 4f. As expected, MTBE adsorption capacity increased with initial MTBE concentration, and MTBE removal efficiency declined. At the lowest BAC#3 dose of 2 g/L, MTBE adsorption capacity increased from 4.6 to 10.3 mg/g as MTBE removal decreased from 46% to 30%. A one-way ANOVA test shows that MTBE removal increases with decreasing initial MTBE concentrations (p-value < 0.001), because sufficient adsorption sites are available for MTBE absorption. Conversely, the adsorption capacity of BAC#3 increased with increasing initial MTBE concentration as there is a higher driving force for absorption due to the higher MTBE concentration.

3.3. ANN modeling

MATLAB (The Mathworks, Inc., 2012) software was chosen to generate neural network model. Preprocessing of the inputs and targets was done by normalizing them in the range of 0 to 1 using 'PREMNMX' function to make the neural network training more efficient. Hyperbolic tangent 'TANSIG' (being a sigmoid transfer function) was chosen for the input to hidden layer map-ping, while a purely linear transfer function 'PURELIN' was chosen for the hidden layer to the output layer mapping. To obtain the objective model, the data points including inputs and their corresponding outputs were split into three random sets: 70% used for developing the new model, 15% used for validation and the last 15% used for testing the model reliability. The reporting ability of feed-forward architecture of ANN also known as multilayer perceptron with back-propagation algorithm was selected and trained in this study.

In this study, a trial and error procedure in respect of cross-validation was used to select the optimal number of hidden layers. For this purpose, we started with one hidden layer and then the neural network is trained and tested. The hidden layer number is then increased and the process is repeated while the overall results of the training and testing are improved (Fig. 5a).

The optimal architecture of the ANN model was obtained based on the highest R^2 and lowest MSE value of testing data set. Therefore, the value of 5 for hidden layer was selected as an optimum case. The MSE vs. the number of epochs for optimal ANN models (Fig. 5b) show that the training was stopped after 31 epochs.

The plotting of predicted removal data for the training and testing (Fig. 5c) indicates good agreement between experimental and predicted data. The value of R^2 for ANN model was found to be 0.99.

3.4. Isotherm study

Adsorption experiments were carried out by batch systems to obtain MTBE concentrations in the liquid phase. Several adsorption models can be used to describe experimental data of adsorption isotherms. According to Table 2, the equilibrium data were modeled with the Freundlich [22], Langmuir [23], Temkin [24], Dubinin–Radushkevich (D-R) [25], Generalized [26], and Redlich–Peterson (R-P) [27] isotherms (Eqs. (11)–(19)). This study aimed to find the best isotherm model that can correctly predict MTBE removal and equilibrium liquid phase concentration. In order to fit the experimental and predicted values of adsorption capacity for plotting the isotherm curves, average percentage errors (APE) were calculated according to Eq. (8).

$$\mathrm{APE}(\%) = \frac{\sum_{i=1}^{N}\left|\frac{q_{e(\exp)} - q_{e(p)}}{q_{e(\exp)}}\right|}{N} \times 100 \tag{8}$$

3.4.1. Freundlich isotherms

The Freundlich isotherm was selected to estimate the MTBE adsorption capacity using BAC#3. The Freundlich isotherm model proposes monolayer adsorption with a heterogeneous distribution of active sites, accompanied by interactions between adsorbed molecules [22]. It can be derived assuming a logarithmic decrease in the enthalpy of sorption with an increase in the fraction of occupied sites [26]. The calculated parameters of the linear Freundlich isotherm models for MTBE adsorption on BAC#3 are presented in Table 3. The $1/n$ values were between 0 and 1 indicating that the adsorption of MTBE on BAC#3 was favorable. The values of $1/n$ were found to be 0.52, 0.57, 0.69, 0.69, and 0.76 for MTBE adsorption at BAC#3 concentrations of 2, 3, 4, 5, and 6 g/L, respectively. The APE values were 3.65, 0.3.04, 1.75, 2.84, and 2.8, respectively, indicating that the linear Freundlich model was able to adequately describe the relationship between the amount of adsorbed MTBE on BAC#3 and its equilibrium concentration in solution.

The distribution coefficient, K_D (m^3/kg), reflects the binding ability of an adsorbent surface for an element and confirms the outcome from the Freundlich isotherm. The K_D value of a system mainly depends on the pH and surface type. K_D values for MTBE and BAC#3 at solution pH 4 were calculated with Eq. (9).

$$K_D = \frac{C_{ss}}{C_w} \tag{9}$$

The value of K_D decreases with rising BAC#3 dosages which demonstrate the heterogeneous surface of BAC#3. When an adsorbent surface is homogeneous, K_D values at a given pH should not change with adsorbent dosage.

3.4.2. Langmuir isotherm

The Langmuir isotherm is used to obtain the maximum adsorption capacity produced from complete monolayer coverage of an adsorbent surface [23]. The Langmuir model represents one of the first theoretical treatments of non-linear sorption and suggests that uptake occurs on a homogeneous surface by monolayer sorption without interaction between adsorbed molecules. In addition, the model assumes uniform adsorption energies onto the adsorbent surface and also no

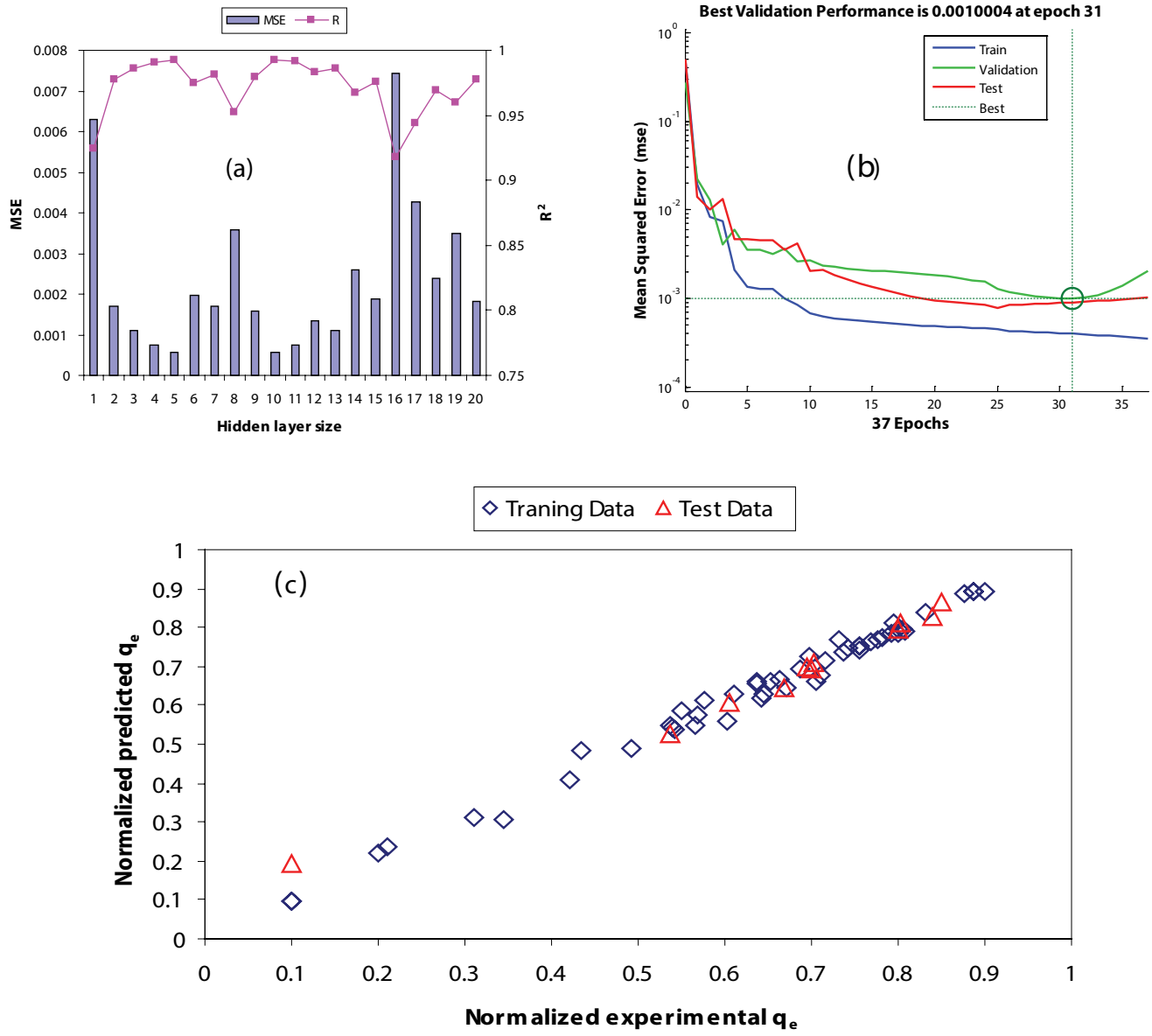

Fig. 5. Optimization of number of hidden layer base on MSR and R^2 (a), MSE vs. the number of epochs (b) and experimental data vs. the predicted data of normalized removal from ANN (c).

transmigration of the adsorbate [26]. The Langmuir isotherm can be linearized as four different types (Table 2), and simple linear regression will result in different parameter estimates. MTBE adsorption isotherms parameters are summarized in Table 3. The APE results show that the adsorption of MTBE by BAC#3 follows the Langmuir-1 type and does not follow the other three types. The applicability of the Langmuir-1 type to the MTBE adsorption with BAC#3 was proven by APE for all tested BAC#3 dosages. According to the literature [9], the essential features of the Langmuir isotherm can be expressed in terms of a dimensionless separation factor or equilibrium parameter, R_L, which is defined according to Eq. (10).

$$R_L = \frac{1}{1+\left(K_L C_0\right)} \tag{10}$$

The values of R_L indicate the type of isotherm to be irreversible (R_L = 0), favorable (0 < R_L < 1), linear (R_L = 1), or unfavorable (R_L > 1). R_L values varied from 0.29 to 0.79 indicating favorable adsorption.

3.4.3. Temkin isotherm

The Temkin model was also used to describe MTBE adsorption onto BAC#3. The Temkin model considers the effects of indirect adsorbate/adsorbate interactions whereby the heat of adsorption of all the adsorbate molecules on the adsorbent surface layer would decrease linearly with coverage due to adsorbate–adsorbate interactions rather than logarithmically, as implied in the Freundlich equation [26]. The values of A_T and B_T for all BAC#3 dosages are presented

Table 2
Non-linear and linear forms of studied isotherm model

Isotherms	Equation	Linear form	
Freundlich	$q_e = K_f C_e^{1/n}$	$\log q_e = \log K_f + \left(\frac{1}{n}\right)\log C_e$	(11)
Langmuir – 1	$q_e = \frac{Q_m K_L C_e}{1 + K_L C_e}$	$\frac{C_e}{q_e} = \left(\frac{1}{K_L Q_m}\right) + \left(\frac{1}{Q_m}\right) C_e$	(12)
Langmuir – 2		$\frac{1}{q_e} = \frac{1}{Q_m} + \left(\frac{1}{K_L Q_m}\right)\frac{1}{C_e}$	(13)
Langmuir – 3		$q_e = Q_m - \left(\frac{1}{K_L}\right)\frac{q_e}{C_e}$	(14)
Langmuir – 4		$\frac{q_e}{C_e} = K_L Q_m - K_L q_e$	(15)
Temkin	$q_e = \frac{RT}{b}\ln\left(A_T C_e\right)$	$q_e = B_T \ln A_T + B_T \ln C_e$	(16)
D-R	$q_e = Q_m \exp\left(-K_{D-R}\varepsilon^2\right)$ $\varepsilon = RT\ln\left(1 + \frac{1}{C_e}\right)$	$\ln q_e = \ln Q_m - K_{D-R}\varepsilon^2$	(17)
Generalized	$q_e = \frac{C_e^{N_b} Q_m}{C_e^{N_b} + K_G}$	$\log\left(\frac{Q_m}{q_e} - 1\right) = \log K_G - N_b \log C_e$	(18)
R-P	$q_e = \frac{AC_e}{1 + BC_e^g}$	$\ln\left(A\frac{C_e}{q_e} - 1\right) = g\ln C_e + \ln B$	(19)

in Table 3. The Temkin constants were used to calculate the heat of adsorption (b) given by Eq. (20).

$$B_T = \frac{RT}{b} \tag{20}$$

As seen in Table 3, the variation of adsorption energy, $b = (-\Delta H)$, is positive for all BAC#3 dosages, which indicates that the adsorption reaction is exothermic.

3.4.4. Dubinin–Radushkevich (D-R) isotherm

The D-R equation, based on Polanyi's potential theory of physical adsorption has been used to estimate the adsorption capacity for volatile organic compounds on microporous adsorbents such as activated carbon [28]. The equation has a semi-empirical origin and is based on the assumptions of a change in the potential energy between a volatile compound and adsorbed phases and a characteristic energy of a given solid. It does not assume a homogeneous surface or a constant sorption potential [1]. This equation yields a macroscopic behavior of adsorption loading for a given pressure [29]. The D-R model was chosen to estimate the characteristic porosity and the apparent free energy of adsorption [26]. The D-R adsorption isotherm model is temperature independent and more general than the Freundlich and Langmuir models. The constants obtained from the plot of the D-R model are shown in Table 3. The adsorption capacity (q_m) of MTBE was 12.6, 9.1, 8.1, 7.2, and 6.6 mg/g with BAC#3 dosages of 2, 3, 4, 5, and 6 g/L and initial MTBE concentrations of 20–70 mg/L at pH 4. The biosorption mean free energy gives information about the biosorption mechanism. The sorption energy (E) for MTBE adsorption onto BAC#3 is calculated using Eq. (21).

$$E = \frac{1}{\sqrt{\left(-2K_{D-R}\right)}} \tag{21}$$

If the E value is between 8 and 16 kJ/mol, the biosorption process follows by chemical ion-exchange; if E < 8 kJ/mol, the biosorption process is of a physical nature [26]. According to Table 3, mean biosorption energy was found to be 10.4,

Table 3
Isotherm parameters obtained using the linear and non-linear method from the various isotherm models for adsorption of MTBE onto BAC #3

Method type	Isotherm	Parameter	Dose of BAC #3 (g/L)				
			2	3	4	5	6
Linear method	Freundlich	$1/n$	0.518	0.573	0.692	0.693	0.759
		K_F	1.421	0.837	0.481	0.421	0.304
		APE (%)	3.69	3.04	1.75	2.84	2.80
	Langmuir-1	Q_m	15.49	12.56	14.56	11.89	13.17
		K_L	0.041	0.031	0.018	0.020	0.015
		APE (%)	2.34	2.95	3.65	2.89	2.77
	Langmuir-2	Q_m	15.77	11.76	12.11	11.96	12.76
		K_L	0.039	0.035	0.024	0.020	0.015
		APE (%)	2.34	2.88	3.14	2.85	15.33
	Langmuir-3	Q_m	15.34	11.81	12.92	10.89	11.95
		K_L	0.041	0.035	0.022	0.023	0.017
		APE (%)	2.39	2.77	3.48	3.54	3.71
	Langmuir-4	Q_m	15.71	12.43	14.22	13.27	11.97
		K_L	0.039	0.031	0.019	0.020	0.015
		APE (%)	2.33	2.86	3.71	11.12	9.62
	Temkin	A_T	0.326	0.269	0.205	0.218	0.197
		B_T	3.720	2.899	2.875	2.418	2.308
		b	663.779	851.762	858.872	1,021.199	1,069.869
		APE (%)	2.11	3.38	6.46	3.88	5.10
	D-R	Q_m	12.589	9.091	8.137	7.154	6.561
		$K_{D\text{-}R}$	-4.62×10^{-3}	4.89×10^{-3}	5.52×10^{-3}	5.57×10^{-3}	5.89×10^{-3}
		E	10.399	10.119	9.510	9.473	9.212
		APE (%)	2.37	4.64	7.02	4.52	5.82
	Generalized	N_b	0.535	0.399	0.444	0.341	0.275
		K_G	37.46	25.06	26.12	20.24	19.44
		APE (%)	72.90	67.75	61.74	58.44	55.63
	R-P	A	0.631	0.612	0.731	0.823	0.900
		g	0.982	0.679	0.419	0.3843	0.288
		B	0.043	0.207	0.799	1.23	2.144
		APE (%)	2.403	2.52	2.02	2.82	2.73
Non-linear method	Freundlich	$1/n$	0.501	0.573	0.717	0.682	0.759
		K_F	1.51	0.838	0.443	0.436	0.304
		APE (%)	3.73	3.05	1.88	2.89	2.81
	Langmuir	Q_m	15.602	13.042	16.898	12.341	14.471
		K_L	0.039	0.029	0.015	0.019	0.013
		APE (%)	2.31	3.12	3.45	2.75	2.87
	Temkin	A_T	0.319	0.258	0.200	0.212	0.189
		B_T	3.757	2.965	2.934	2.465	2.375
		APE (%)	2.05	3.66	6.90	4.20	5.63
	D-R	Q_m	12.944	9.803	9.177	7.715	7.325
		$K_{D\text{-}R}$	-4.92×10^{-3}	-5.68×10^{-3}	-6.67×10^{-3}	-6.31×10^{-3}	-6.96×10^{-3}
		E	10.084	9.386	8.658	8.900	8.478
		APE (%)	3.02	5.71	8.37	6.09	7.18
	Generalized	N_b	1.001	0.984	0.977	0.400	0.291
		K_G	25.193	33.177	63.480	21.34	20.11
		APE (%)	2.69	2.25	28.80	53.62	55.23
	R-P	A	0.609	0.882	16.171	0.394	0.897
		g	1.000	0.565	0.286	0.541	0.287
		B	0.035	0.508	35.732	0.262	2.145
		APE (%)	2.271	2.68	1.89	2.70	2.73

10.1, 9.5, 9.5, and 9.2 kJ/mol at BAC#3 dosages of 2, 3, 4, 5, and 6 g/L, respectively. The results demonstrate that the adsorption of MTBE onto BAC#3 may be performed according to a chemical ion-exchange mechanism (8–16 kJ/mol).

3.4.5. Generalized isotherm

Classical isotherms of adsorption are based on the model of an impenetrable interface, where an adsorbate can substitute only one molecule for one solvent molecule. However, at the interface between two immiscible electrolytes, similar to a nonpolar oil–water interface or a liquid membrane, amphiphilic molecules can substitute molecules in both solvents; therefore, classical isotherms are not applicable in these cases. A generalized isotherm model was tested for correlation of the equilibrium data. As depicted in Table 3, the generalized adsorption isotherm did not result in a good fit to the experimental data. The cooperative binding constant (N_b) value was calculated to be 0.54, 0.4, 0.31, and 0.28 at BAC3# doses of 2, 3, 4, 5, and 6 g/L, respectively.

3.4.6. Redlich–Peterson (R-P) isotherm

The R-P is one of three parameter isotherms and incorporates the features of the Langmuir and Freundlich isotherms. The R-P isotherm has a linear dependence on concentration in the numerator and an exponential function in the denominator. At low concentrations, the R-P isotherm approximates to Henry's law and at high concentrations, its behavior approaches that of the Freundlich isotherm [30]. Furthermore, the R-P equation incorporates three parameters into an empirical isotherm, and therefore, can be applied either in homogenous or heterogeneous systems making it highly versatile. Fig. 6a shows the isotherm plots of the R-P isotherms and isotherm parameters are shown in Table 3. In all cases, APE values were <3% which shows a good applicability of this model for the adsorption of MTBE using BAC#3. In addition, as seen in Table 3, the g value almost reaches 1.0 at the 2 g/L dose which suggests the isotherm is approaching the Langmuir form.

3.5. Non-linear isotherms method

Nowadays, application of nonlinear procedures is going to very popular, for example, for kinetics and isotherm calculation in chemistry field and pharmacokinetic in the medicine field. Currently non-linear regression method is found to be the best way in selecting the optimum isotherm. Also, non-linear method has an advantage that the error distribution does not get altered as in linear technique, as all the coefficient parameters are fixed in the same axis. In this study, for non-linear methods, the solver function on MS Excel was used to fit the adsorption equations to the experimental data (Table 3). The isotherm parameters obtained from the non-linear methods differed slightly even with the methods having the lowest APE values. The best fit was obtained by the R-P isotherm. Fig. 7 shows non-linear isotherms fitted to the experimental data.

3.6. Kinetic study

Adsorption kinetic parameters are useful for the prediction of the adsorption rate and gives important information for designing adsorption systems and modeling the process [31]. In order to investigate the mechanism of biosorption and potential rate controlling steps such as mass transport and chemical reaction processes, kinetic models have been used to test experimental data [30]. In the present study, the kinetic models of pseudo-first order [26], pseudo-second order [32], Elovich [33], and intraparticle diffusion [34] were used to analyze the MTBE adsorption kinetics data according to Eqs. (22) as summarized in Table 4. The applicability of a particular model for the MTBE–BAC#3 system was evaluated from goodness of fit, the correlation coefficient (R^2), and a comparison of experimental and predicted amounts of MTBE adsorbed at equilibrium q_e (mg/g).

3.6.1. Pseudo-first order model

The pseudo-first order kinetic model has been widely used to predict sorption kinetics. The kinetic data were treated with the Lagergren first order model [26], which is the earliest model known describing the adsorption rate based on the adsorption capacity. The model given by Lagergren and Svenska is shown in Table 4. The rate variation should be proportional to the first power of concentration for strict surface adsorption. However, the relationship between initial solute concentration and the rate of adsorption will not be linear when pore diffusion limits the adsorption process.

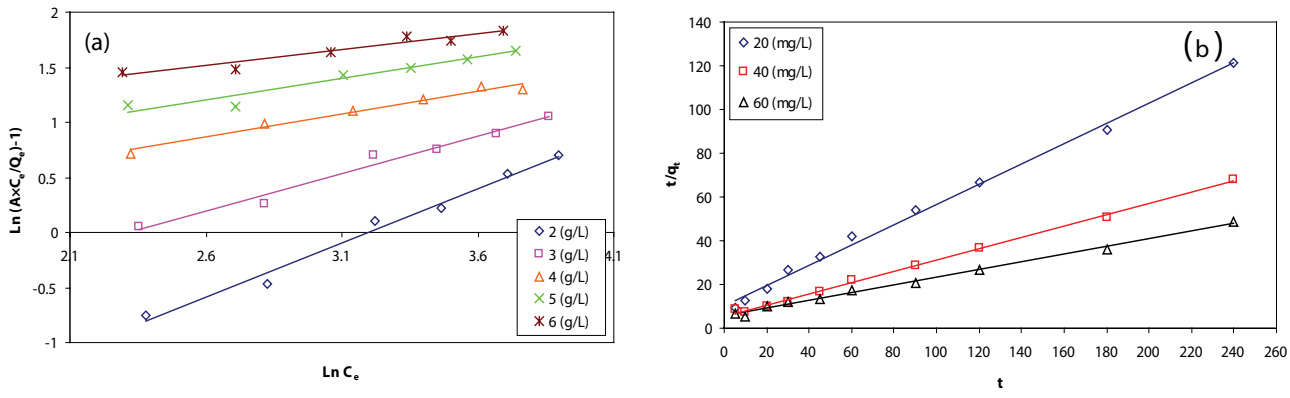

Fig. 6. Plot of the R-P isotherm (a) and type 1 of pseudo-second-order model (b).

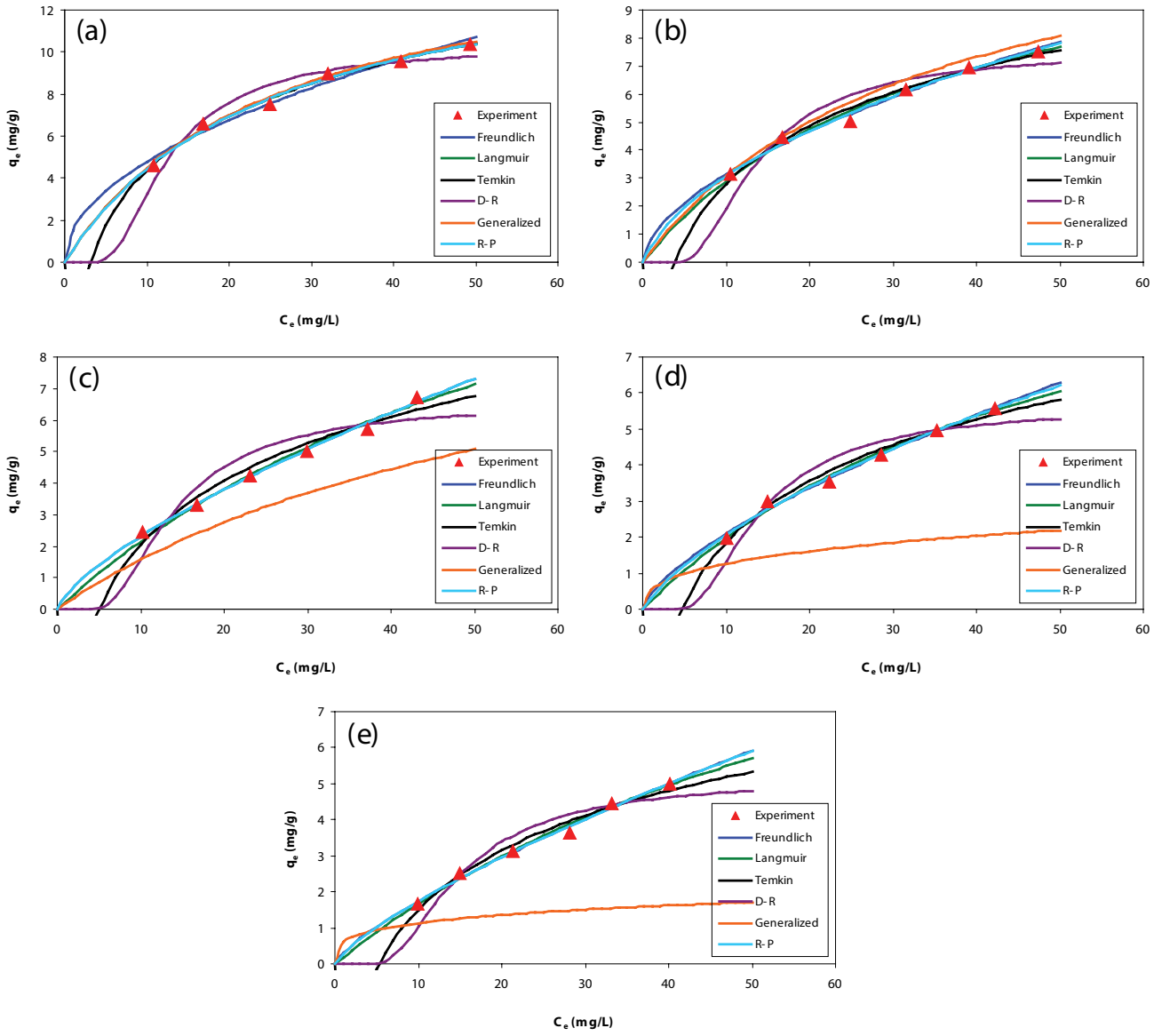

Fig. 7. Isotherms obtained using the non-linear method for MTBE adsorption onto BAC#3: (a) 2, (b) 3, (c) 4, (d) 5, and (e) 6 g/L dose.

The values of the kinetic parameters and the R^2 values obtained are given in Table 5. The R^2 values were >0.93 for initial MTBE concentrations of 20–60 mg/L.

3.6.2. Pseudo-second order model

An expression of the pseudo-second order rate equation depends on the sorption capacity on the solid phase. The pseudo-second order kinetic model could be linearized to four different types (Table 4); the most popular linear form used is type 1. The linear plots of the type 1 pseudo-second order model showed good agreement between the experimental and calculated q_e values at different initial MTBE concentrations (Fig. 6b). In contrast to the other kinetic models, the R^2 values were ≥0.99 which indicates that the type 1 pseudo-second order kinetic model provided good correlation for MTBE adsorption by BAC#3 for all MTBE concentrations (Table 5). The initial sorption rate (h) increased from 0.1 to 0.2 as the initial MTBE concentration increased from 20 to 60 mg/L according to Eq. (22).

$$h = k_2 q_e^2 \tag{22}$$

3.6.3. Elovich model

The Elovich kinetic equation is another rate equation based on adsorption capacity and one of the most useful models for describing activated chemisorptions. In this case, the linear correlation coefficients were highly significant (>0.96) and once more demonstrated a high degree of correlation between the experimental data and the theoretical data predicted by the Elovich model (Table 5). As represented in Table 4, the values of α and β varied as a function of the initial

Table 4
Non-linear and linear forms of studied kinetic model

Kinetic models	Equation	Linear form	
Pseudo first order	$\frac{dq_t}{dt} = k_1\left(q_e - q_t\right)$	$\log\left(q_e - q_t\right) = \log\left(q_e\right) - \frac{k_1}{2.303}t$	(22)
Pseudo-second order; type 1		$\frac{t}{q_t} = \left(\frac{1}{k_2 q_e^2}\right) + \left(\frac{1}{q_e}\right)t$	(23)
Pseudo-second order; type 2	$\frac{dq_t}{dt} = k_2\left(q_e - q_t\right)^2$	$\frac{1}{q_t} = \left(\frac{1}{k_2 q_e^2}\right)\frac{1}{t} + \frac{1}{q_e}$	(24)
Pseudo-second order; type 3		$q_t = q_e - \left(\frac{1}{k_2 q_e^2}\right)\frac{q_t}{t}$	(25)
Pseudo-second order; type 3		$\frac{q_t}{t} = k_2 q_e^2 - k_2 q_e q_t$	(26)
Elovich	$\frac{dq_t}{dt} = \alpha\exp\left(-\beta q_t\right)$	$q_e = \left(\frac{1}{\beta}\right)\ln\left(\alpha\beta\right) + \left(\frac{1}{\beta}\right)\ln t$	(27)
Intraparticle diffusion	–	$q_t = K_{\text{dif}} t^{0.5} + C$	(28)

Table 5
Parameters obtained from various kinetics models using different MTBE concentrations

Kinetic models	Parameter	MTBE concentration (mg/L)		
		20	40	60
Pseudo-first order	k_1	0.017	0.019	0.02
	$q_{e\,\text{cal}}$	1.39	2.32	4.24
	R^2	0.98	0.93	0.98
Pseudo-second order:	k_2	0.021	0.012	0.006
type 1	$q_{e\,\text{cal}}$	2.16	3.88	5.68
	h	0.098	0.181	0.194
	R^2	0.99	0.99	0.99
Pseudo-second order:	k_2	0.047	0.006	5×10^{-7}
type 2	$q_{e\,\text{cal}}$	1.85	4.89	5.70
	h	0.145	0.137	0.186
	R^2	0.98	0.96	0.96
Pseudo- second order:	k_2	0.036	0.012	0.007
type 3	$q_{e\,\text{cal}}$	1.94	3.38	5.21
	h	0.134	0.183	0.214
	R^2	0.91	0.84	0.83
Pseudo-second order:	k_2	0.031	0.010	0.190
type 4	$q_{e\,\text{cal}}$	1.99	4.12	5.60
	h	0.125	0.164	0.190
	R^2	0.91	0.84	0.83
Elovich	α	0.52	1.25	2.93
	β	2.56	1.31	0.88
	R^2	0.98	0.96	0.97
Intraparticle diffusion	K_{dif}	0.108	0.199	0.314
	C	0.53	0.95	0.79
	R^2	0.93	0.81	0.92

MTBE concentration. With increasing MTBE initial concentration from 20 to 60 mg/L, the value of α increased from 0.5 to 2.9 (mg/g-min) and the value of β decreased from 2.56 to 0.88 g/mg.

3.6.4. Intraparticle diffusion model

As the above kinetic models are not able to identify the diffusion mechanism, understanding the underlying mechanism of adsorption and the rate controlling step is important for determining an appropriate residence time which is essential for good process design and control of adsorption treatment systems. The results of intraparticle diffusion kinetics are described in Table 5. The values of C provide information about the thickness of the boundary layer – the resistance to the external mass transfer increases as the intercept increases (Table 5). The values of C were augmented with rising initial MTBE concentration, indicating the increase of the thickness of the boundary layer and the decrease of the chance of external mass transfer and hence an increase of the chance of internal mass transfer. For MTBE adsorption onto BAC#3, the intercept was passed through the origin proposing that even though the adsorption process involved intraparticle diffusion, it was the only rate-controlling step.

4. Conclusion

Adsorption studies performed on activated carbon derived from WAS revealed the ability of bioactivated carbon to remove MTBE from aqueous phase. According to obtained results, the following results can be concluded as:

- The FTIR spectra of WAS and BAC was depicted that the C–H and C–C were major surface functional groups.

- Type of chemical activation of WAS has a significant influence on MTBE adsorption.
- BAC#3 micrograph was containing the different sizes and shapes of pores, which resulted from the evaporation of $ZnCl_2$ during carbonization.
- Batch sorption studies performed on the MTBE–BAC sorption system indicated varied MTBE adsorption capacity.
- The D-R isotherm demonstrated that the adsorption of MTBE onto BAC#3 may be performed according to a chemical ion-exchange mechanism (8–16 kJ/mol).
- The adsorption reaction was fitted well using the pseudo-second order kinetic model (type 1).
- Examination of ANN modeling depicted high Pearson correlation valve and low MSE and demonstrated that ANN models are more efficient for explaining adsorption behaviors of MTBE onto BAC#3.

Acknowledgment

The authors would like to acknowledge the financial support of the "Isfahan University of Medical Sciences" through the Project#290269.

Symbols

A — Redlich Peterson isotherm constant, L/g
APE — Average percentage errors
AT — Temkin constant, L/g
B — Redlich Peterson isotherm constant, $L/mg^{1-(1/A)}$
BT — Constant related to heat of adsorption, mg/L
C — Thickness of the boundary layer, mg/g
C_0 — Initial concentration, mg/L
C_e — Equilibrium concentration in solution, mg/L
C_s — Saturation concentration in solution, mmol/L
C_{ss} — Concentration of adsorbate on adsorbent, mg/kg
C_t — Equilibrium concentration in solution at time t, mg/L
C_w — Equilibrium concentration in solution, mg/m^3
E — Adsorption mean free energy, kJ/mol
g — Redlich–Peterson constant
h — Initial sorption rate, mg/g min
k_1 — Pseudo-first-order rate constant, 1/min
k_2 — Pseudo-second-order rate constant, g/mg min
K_D — Distribution coefficient
K_{dif} — Intraparticle diffusion rate constant, $mg/g\ min^{0.5}$
$K_{D\text{-}R}$ — Adsorption energy, mol^2/kJ^2
K_f — Maximum adsorption capacity, mg/g
K_G — Saturation constant, mg/L
K_L — Langmuir isotherm constants, L/mg
m — Mass of adsorbent, g
n — Freundlich exponent
N — Number of experimental data
N_b — Cooperative binding constant
q_e — Equilibrium adsorbent concentration on adsorbent, mg/g
$q_{e\ cal}$ — Calculated values of q_e, mg/g
$q_{e(exp)}$ — Equilibrium capacity of experiment, mg/g
$\overline{q_{e(exp)}}$ — Average of $q_{e(exp)}$, mg/g
Q_m — Maximum monolayer capacity, mg/g
$q_{e(p)}$ — Predicted equilibrium capacity
q_t — Adsorbed concentration at time t, mg/g
R — Universal gas constant, 8.314 J/mol K
R^2 — Correlation coefficient
r^2 — Pearson coefficient
R_L — Dimensional separation factor
T — Absolute temperature, K
V — Volume of liquid in reactor, L
α — Initial adsorption rate, mg/g min
β — Desorption constant, g/mg
ε — Polanyi potential
$y_{pre,i}$ — Predicted value by ANN model
$y_{exp,i}$ — Experimental value
y_{ave} — Average of the experimental value

References

[1] S.K. Ghadiri, R. Nabizadeh, A.H. Mahvi, S. Nasseri, H. Kazemian, A.R. Mesdaghinia, S. Nazmara, Methyl tert-butyl ether adsorption on surfactant modified natural zeolites, Iran. J. Environ. Health Sci. Eng., 7 (2010) 241–252.
[2] A. Fischer, M. Müller, J. Klasmeier, Determination of Henry's law constant for methyl tert-butyl ether (MTBE) at groundwater temperatures, Chemosphere, 54 (2004) 689–694.
[3] N. Kuburovic, M. Todorovic, V. Raicevic, A. Orlovic, L. Jovanovic, J. Nikolic, V. Kuburovic, S. Drmanic, T. Solevic, Removal of methyl tertiary butyl ether from wastewaters using photolytic, photocatalytic and microbiological degradation processes, Desalination, 213 (2007) 123–128.
[4] T.-N. Wu, Electrochemical removal of MTBE from water using the iridium dioxide coated electrode, Sep. Purif. Technol., 79 (2011) 216–220.
[5] B. Burghoff, J. Sousa Marques, B.M. van Lankvelt, A.B. de Haan, Solvent impregnated resins for MTBE removal from aqueous environments, React. Funct. Polym., 70 (2010) 41–47.
[6] J. Lu, F. Xu, D. Wang, J. Huang, W. Cai, The application of silicalite-1/fly ash cenosphere (S/FAC) zeolite composite for the adsorption of methyl tert-butyl ether (MTBE), J. Hazard. Mater., 165 (2009) 120–125.
[7] E.M. Seeger, P. Kuschk, H. Fazekas, P. Grathwohl, M. Kaestner, Bioremediation of benzene-, MTBE- and ammonia-contaminated groundwater with pilot-scale constructed wetlands, Environ. Pollut., 159 (2011) 3769–3776.
[8] M. Ghasemian, M.M. Amin, E. Morgenroth, N. Jaafarzadeh, Anaerobic biodegradation of methyl tert-butyl ether and tert-butyl alcohol in petrochemical wastewater, Environ. Technol., 33 (2012) 1937–1943.
[9] M. Malakootian, A. Fatehizadeh, N. Yousefi, M. Ahmadian, M. Moosazadeh, Fluoride removal using Regenerated Spent Bleaching Earth (RSBE) from groundwater: Case study on Kuhbonan water, Desalination, 277 (2011) 244–249.
[10] M. Aivalioti, D. Pothoulaki, P. Papoulias, E. Gidarakos, Removal of BTEX, MTBE and TAME from aqueous solutions by adsorption onto raw and thermally treated lignite, J. Hazard. Mater., 207–208 (2012) 136–146.
[11] A. Rossner, D.R.U. Knappe, MTBE adsorption on alternative adsorbents and packed bed adsorber performance, Water Res., 42 (2008) 2287–2299.
[12] B. Ji, F. Shao, G. Hu, S. Zheng, Q. Zhang, Z. Xu, Adsorption of methyl tert-butyl ether (MTBE) from aqueous solution by porous polymeric adsorbents, J. Hazard. Mater., 161 (2009) 81–87.
[13] L. Abu-Lail, J.A. Bergendahl, R.W. Thompson, Adsorption of methyl tertiary butyl ether on granular zeolites: batch and column studies, J. Hazard. Mater., 178 (2010) 363–369.
[14] M. Aivalioti, P. Papoulias, A. Kousaiti, E. Gidarakos, Adsorption of BTEX, MTBE and TAME on natural and modified diatomite, J. Hazard. Mater., 207–208 (2012) 117–127.
[15] S.W. Davis, S.E. Powers, Alternative sorbents for removing MTBE from gasoline-contaminated ground water, J. Environ. Eng., 126 (2000) 354–360.

[16] V.M. Monsalvo, A.F. Mohedano, J.J. Rodriguez, Activated carbons from sewage sludge: application to aqueous-phase adsorption of 4-chlorophenol, Desalination, 277 (2011) 377–382.
[17] M. Molina-Sabio, F. Rodríguez-Reinoso, Role of chemical activation in the development of carbon porosity, Colloids Surf., A, 241 (2004) 15–25.
[18] A. Nasrullah, A. Bhat, M.H. Isa, M. Danish, A. Naeem, N. Muhammad, T. Khan, Efficient removal of methylene blue dye using mangosteen peel waste: kinetics, isotherms and artificial neural network (ANN) modelling, Desal. Wat. Treat., 86 (2017) 191–202.
[19] J. Gómez-Sanchis, J.D. Martín-Guerrero, E. Soria-Olivas, J. Vila-Franc'es, J.L. Carrasco, S.d. Valle-Tascón, Neural networks for analysing the relevance of input variables in the prediction of tropospheric ozone concentration, Atmos. Environ.., 40 (2006) 6173–6180.
[20] U. Özdemir, B. Özbay, S. Veli, S. Zor, Modeling adsorption of sodium dodecyl benzene sulfonate (SDBS) onto polyaniline (PANI) by using multi linear regression and artificial neural networks, Chem. Eng. J., 178 (2011) 183–190.
[21] G. Bonyadinejad, M. Sarafraz, M. Khosravi, A. Ebrahimi, S.M. Taghavi-Shahri, R. Nateghi, S. Rastaghi, Electrochemical degradation of the Acid Orange 10 dye on a Ti/PbO_2 anode assessed by response surface methodology, Korean J. Chem. Eng., 33 (2016) 189–196.
[22] H.M.F. Freundlich, Uber die adsorption in losungen, J. Phys. Chem. A, 57 (1906) 385–470.
[23] I. Langmuir, The constitution and fundamental properties of solids and liquids, J. Am. Chem. Soc., 38 (1916) 2221–2295.
[24] M. Temkin, J.A.V. Pyzhev, Kinetics of ammonia synthesis on promoted Iron catalysts, Acta Physicochim. URSS, 12 (1940) 217–229.
[25] M.M. Dubinin, E.D. Zaverina, L.V. Radushkevich, Sorption and structure of active carbons I. Adsorption of organic vapors, Zh. Fiz. Khim., 21 (1947) 1351–1362.
[26] A.E. Nemr, Potential of pomegranate husk carbon for Cr(VI) removal from wastewater: kinetic and isotherm studies, J. Hazard. Mater., 161 (2009) 132–141.
[27] O. Redlich, D.L. Peterson, A useful adsorption isotherm, J. Phys. Chem., 63 (1959) 1024–1025.
[28] M. Jahandar Lashaki, M. Fayaz, S. Niknaddaf, Z. Hashisho, Effect of the adsorbate kinetic diameter on the accuracy of the Dubinin–Radushkevich equation for modeling adsorption of organic vapors on activated carbon, J. Hazard. Mater., 241–242 (2012) 154–163.
[29] C. Nguyen, D.D. Do, The Dubinin-Radushkevich equation and the underlying microscopic adsorption description, Carbon, 39 (2001) 1327–1336.
[30] Z. Aksu, Determination of the equilibrium, kinetic and thermodynamic parameters of the batch biosorption of nickel(II) ions onto *Chlorella vulgaris*, Process Biochem., 38 (2002) 89–99.
[31] M. Ahmadian, N. Yousefi, A. Toolabi, N. Khanjani, S. Rahimi, A. Fatehizadeh, Adsorption of direct yellow 9 and acid orange 7 from aqueous solutions by modified pumice, Asian J. Chem., 24 (2012) 3094–3098.
[32] Y. Khambhaty, K. Mody, S. Basha, B. Jha, Pseudo-second-order kinetic models for the sorption of Hg(II) onto dead biomass of marine *Aspergillus niger*: comparison of linear and non-linear methods, Colloids Surf., A, 328 (2008) 40–43.
[33] S.H. Chien, W.R. Clayton, Application of Elovich equation to the kinetics of phosphate release and sorption on soils, Soil Sci. Soc. Am. J., 44 (1980) 265–268.
[34] W.J. Weber, J.C. Morris, Kinetics of adsorption on carbon from solution, J. Sanit. Eng. Div., 89 (1963) 31–60.